Aurora A Is Critical for Survival in HPV-Transformed Cervical Cancer

Brian Gabrielli[1], Fawzi Bokhari[1], Max V. Ranall[1], Zay Yar Oo[1], Alexander J. Stevenson[1], Weili Wang[1], Melanie Murrell[2], Mushfiq Shaikh[2], Sora Fallaha[2], Daniel Clarke[2], Madison Kelly[2], Karin Sedelies[3], Melinda Christensen[3], Sara McKee[1], Graham Leggatt[1], Paul Leo[1], Dubravka Skalamera[1], H. Peter Soyer[4], Thomas J. Gonda[1], and Nigel A.J. McMillan[2]

Abstract

Human papillomavirus (HPV) is the causative agent in cervical cancer. HPV oncogenes are major drivers of the transformed phenotype, and the cancers remain addicted to these oncogenes. A screen of the human kinome has identified inhibition of Aurora kinase A (AURKA) as being synthetically lethal on the background of HPV E7 expression. The investigational AURKA inhibitor MLN8237/Alisertib selectively promoted apoptosis in the HPV cancers. The apoptosis was driven by an extended mitotic delay in the Alisertib-treated HPV E7–expressing cells. This had the effect of reducing Mcl-1 levels, which is destabilized in mitosis, and increasing BIM levels, normally destabilized by Aurora A in mitosis. Overexpression of Mcl-1 reduced sensitivity to the drug.

The level of HPV E7 expression influenced the extent of Alisertib-induced mitotic delay and Mcl-1 reduction. Xenograft experiments with three cervical cancer cell lines showed Alisertib inhibited growth of HPV and non-HPV xenografts during treatment. Growth of non-HPV tumors was delayed, but in two separate HPV cancer cell lines, regression with no resumption of growth was detected, even at 50 days after treatment. A transgenic model of premalignant disease driven solely by HPV E7 also demonstrated sensitivity to drug treatment. Here, we show for the first time that targeting of the Aurora A kinase in mice using drugs such as Alisertib results in a curative sterilizing therapy that may be useful in treating HPV-driven cancers. *Mol Cancer Ther; 14(12); 2753–61. ©2015 AACR.*

Introduction

Human papillomavirus (HPV) has been identified as the definitive agent in cancers of the cervix, penis, vulva, vagina, anus, skin, eye, and head and neck, and is responsible for more than 610,000 deaths, 5% of the total cancer burden worldwide (1). The papillomaviruses are small, double-stranded DNA viruses belonging to the family *Papillomaviridae*. High-risk HPVs have been identified as the causative agent in 99.7% cervical cancers (2), have been detected in more than 50% of other anogenital cancers, and in more than 70% of cancers of the oropharynx (3, 4). The most prevalent high-risk HPV types are HPV-16 and HPV-18, which account for approximately 70% of HPV cancer cases, with another 10 high-risk types making up the other 30% (5).

Although HPV vaccines are available and highly effective (reviewed in ref. 6), they are clearly most useful if given before viral exposure. Even with the advent of vaccines, cervical cancer will remain a serious health issue in unvaccinated and under-vaccinated women (7). The use of more targeted approaches is now beginning to improve outcomes in other cancers but no such therapy for HPV-driven cancers is in the clinic. Indeed, chemo-radiotherapy is still the primary treatment modality and there has been little improvement in 5-year outcomes (8).

High-risk HPV promotes cancer via the actions of the E6 and E7 oncogenes. The E6 gene product binds to the p53 tumor-suppressor protein and targets it for ubiquitin-mediated degradation (9). E6 also blocks senescence by stimulating telomerase activity as well as an increasing number of other proteins (10). The E7 protein also has a range of targets, including the retinoblastoma protein (pRB) family, the MuvB complex, and directly drives genomic instability (10, 11). Therefore, the overexpression of E6 and E7 allows uncontrolled cell growth and increased genomic instability, which promotes transformation and carcinogenesis. This process occurs over an extended timeframe (up to 20 years) due to the fact that E6/E7 alone are not sufficient to drive cancer; secondary mutational events also contribute (12), thus making specific treatment difficult as each HPV cancer has a different spectrum of mutations.

The one consistent feature of cervical cancers is the continued dependence on HPV E6 and E7 expression. Depletion of E6/E7 is sufficient to drive even long established cell lines into either

[1]The University of Queensland Diamantina Institute, Translational Research Institute, Brisbane, Queensland, Australia. [2]Menzies Health Institute Queensland, School of Medical Science, Griffith University, Gold Coast, Queensland, Australia. [3]Mater Research, The University of Queensland, Translational Research Institute, Brisbane, Queensland, Australia. [4]Dermatology Research Centre, School of Medicine, The University of Queensland, Translational Research Institute, Brisbane, Queensland, Australia.

Note: Supplementary data for this article are available at Molecular Cancer Therapeutics Online (http://mct.aacrjournals.org/).

Current address for T.J. Gonda: School of Pharmacy, The University of Queensland, Brisbane, Queensland, Australia.

B. Gabrielli and Fawzi Bokhari contributed equally to this article.

Corresponding Authors: Brian Gabrielli, The University of Queensland, Translational Research Institute, Brisbane, QLD, 4102, Australia. Phone: 61-7-3443-7092; Fax: 61-7-3443-6966; E-mail: brianG@uq.edu.au; and Nigel A.J. McMillan, Molecular Basis of Disease Program, Menzies Health Institute Queensland Griffith University, Gold Coast Campus, Southport, 4222, QLD Australia. E-mail: n.mcmillan@griffith.edu.au

doi: 10.1158/1535-7163.MCT-15-0506

©2015 American Association for Cancer Research.

Gabrielli et al.

senescence or apoptosis, depending on the level of depletion achieved (13). This continuing dependence on E6/E7 suggests that drugs that targeting E6/E7 are also likely to be selective for HPV-transformed cancers. We have undertaken a functional genomics screen to identify genes involved in E6/E7-driven dependency that are essential to the survival of HPV-driven cancers. Here, we show for the first time that targeting of the Aurora A kinase using the inhibitor Alisertib results in a profound inhibition of HPV-driven tumor growth, and that this selectivity is through targeting an interaction between Aurora A and HPV E7 in mitosis.

Materials and Methods

Cell culture

All cervical cancer cell lines were originally obtained from the ATCC except for C33A. Cervical cancer cell lines (HeLa, CaSki, ME-180, SiHa, C33A, HT3, and C33A-HPV16-E7) were maintained in complete DMEM (GIBCO; Invitrogen) supplemented with 10% serum supreme (Biowhittaker; Lonza), 1 mmol/L sodium pyruvate (GIBCO) and 2 mmol/L L-glutamine (GIBCO) at 37°C and 5% CO_2. Squamous cell carcinoma cell lines were kindly given by Associate Professor Nicholas Saunders (The University of Queensland Diamantina Institute, Brisbane, Australia) and were cultured in DMEM/F12 (1:1; GIBCO) containing 10% serum supreme (Lonza) at 37°C and 5% CO_2. All cell lines were tested and free of *Mycoplasma* and authenticated with short tandem repeat fingerprinting at the time of use. SCC25 cells were transduced with lentivirus-expressing HPV18 E7 or empty vector as described previously (14). The vector places the HPV18 E7 5' of an IRES GFP resulting in GFP coexpression at a level, which is an indicator of the level of E7 expression. qPCR analysis of relative E7 gene expression was undertaken using $\Delta\Delta C_t$ analysis and β-actin as the housekeeper.

siRNA screening

Detailed methods for the siRNA screening are provided in Supplementary Material.

Flow cytometry

All tested cells were exposed to final concentrations of 5 μmol/L Alisertib, 5 μmol/L ZM447439, or DMSO (vehicle) for 24, 48, or 72 hours. Cells were analyzed for DNA content by flow cytometry using BD FACS-Canto II (BD Biosciences) and data analyzed with FlowJo software (FlowJo Co.) as described previously (15).

Time-lapse microscopy

Cells were either treated with 5 μmol/L Alisertib or DMSO (vehicle), then followed by time-lapse microscopy using a Zeiss Axiovert 200M Cell Observer microscope equipped with an incubation chamber at 37°C and 5% CO_2. Images were captured at 20 minute intervals with a minimum of 150 cells per condition per cell line analyzed as described previously (15). Time in mitosis and exit from mitosis was observed and assessed for successful cellular division, failure of cytokinesis, or cell death.

Immunoblotting

Cells were lysed and immunoblotted as described previously using chemiluminescence detection imaged with a CCD camera (15). Band intensities were quantitated using ImageJ software. Antibodies to Bim, Bcl-2, PARP, cleaved caspase-3 (Cell Signalling

Technology), Aurora A and Aurora B (Becton-Dickinson), Bcl-Xl (AbCam), Mcl-1 (Millipore), and α-tubulin (Sigma-Aldrich) were purchased from the indicated suppliers.

Mouse xenograft models

Mice (6-weeks-old female Nude; ARC) were inoculated s.c. in the right flank with 1×10^6 cells in Matrigel. For each cell line, 6 mice were used for the treatment with Alisertib and 6 for the vehicle control only. When tumors were palpable (∼1 week following injection) 100 μL oral gavage of 30 mg/kg Alisertib was administered daily for 10 consecutive days. Mice were then scored daily by scoring any tumor regrowth or until culled. All animal studies were approved by University of Queensland Animal Ethics.

K14E7 transgenic mouse grafting experiments

Groups of 7 mice, with well-healed (up to 5 months) grafts of either wild-type or *K14E7* skin were treated with or without two cycles of Alisertib as for the xenograft experiments. At between 2 and 10 days after the final cycle, mice were sacrificed and grafts harvested for immunohistochemical staining. Formalin-fixed, paraffin-embedded samples were either immunostained for cleaved caspase-3 (Cell Signaling Technology) or mast cells using toluidine blue, pH 1. The number of cells stained was visually assessed by microscopy.

Immunofluorescence

Cells were cultured on poly-L-lysine coated glass coverslips with vehicle (DMSO) or 5 μmol/L Alisertib for 24 or 48 hours. Coverslips were fixed with −20°C methanol and stored at −20°C until processing. Coverslips were stained for microtubules and DNA as described previously (16).

qPCR

Extract of RNA, cDNA generation, and qPCR were carried out as described previously described (17).

Results

siRNA library screen and target selection

To discover synthetic lethal interactions with the HPV oncogenes E7 and E6 in cervical cancers, we undertook an siRNA library kinome screen using the Dharmacon human siGENOME siRNA library for Protein Kinases (targeting 779 genes). The primary screen used CaSki (cervical cancer HPV16), and C33A (cervical cancer non-HPV) cell lines. Data were normalized using Z-score transformation for each assay and cell line, and genes sorted by Z-score on CaSki viability. Using the parameters of viability, cytotoxicity, and cell number, we identified genes that when depleted were selectively lethal to the HPV-positive CaSki cell line compared with the HPV-negative C33A cells (Fig. 1A; full screening data presented in Supplementary Table S1). This was visualized using hierarchical clustering and Principle Components Analysis (details of the analysis are provided in Supplementary Fig. S1). We identified a group of genes whose knockdown resulted in reduced viability in all cells, including *PLK1*, *WEE1*, and *COPB2*, which were excluded from further analysis. From this primary screen, we identified a set of 54 genes for secondary screening using the OnTarget Plus siRNA Smart Pools that have reduced off-target effects due to their modified passenger strand and >90% have different target sites
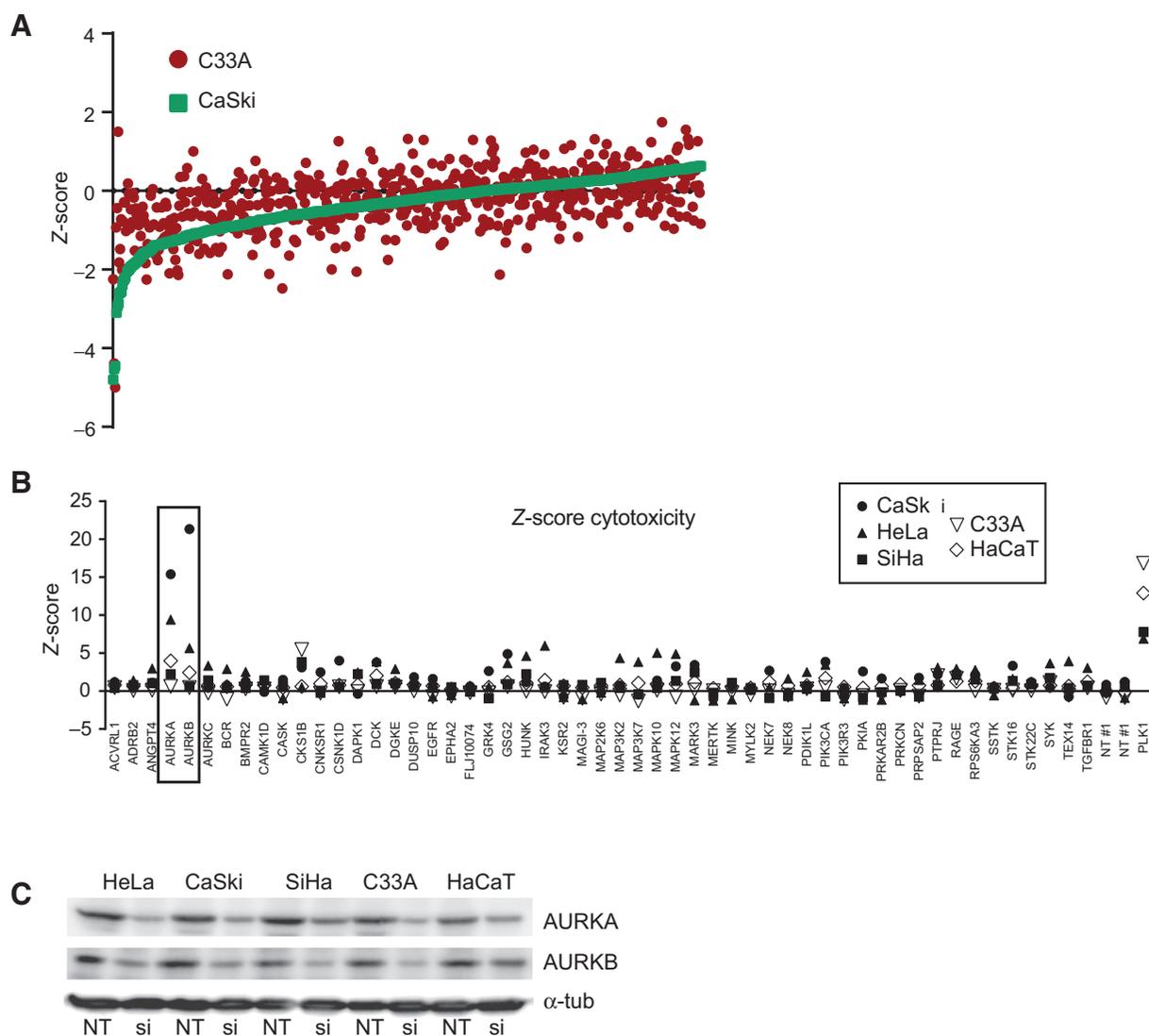
Figure 1.
Kinome siRNA screen of cervical cancer cells. A, cell viability (resazurin) analysis following treatment of CaSki and C33A cells with the Dharmacon Human siGENOME SMARTpool siRNA Library. Each data point represents a mean Z-score of three replicates. B, summary of the top 54 selected hits from the primary screen rescreened using OnTarget Plus siRNA in an expanded panel of cell lines. Only the cytotoxicity data are shown. The top two hits from this validation set are indicated (box). C, cells transfected with either Aurora A kinase (AURKA) or Aurora B kinase (AURKB) ON-Target Plus siRNA and harvested 24 hours after transfection. Nontargeting siRNA (siNT) was used as a control. The levels of Aurora A or B were assayed for the appropriate siRNA, with α-tubulin as a loading control.

(Supplementary Table S2). The secondary screen siRNAs were applied to a larger panel of cell lines including HeLa (HPV18), SiHa (HPV16), and HaCaT (HPV negative) cells using the viability, cytotoxicity, and cell count assay parameters.

From the secondary screen, we identified the genes *AURKA* and *AURKB* as the strongest hits (those with the highest Z-scores) in all three assays (Fig. 1B and Supplementary Fig. S2). Other genes such as *GSG2, SYK, MAPK12, PRKAR2B,* and *STK22C* showed activity in one or two assays, but not in all three. Using Western analysis, we confirmed siRNA depletion of the respective target proteins of our two top hits, Aurora A and Aurora B kinases. Moreover, we observed no obvious differential expression of these proteins in HPV and non-HPV cancer lines (Fig. 1C). With three of the top seven targets (*AURKA, AURKB,* and G*SG2)* acting as regulators of

mitosis it suggested that mitosis may be the common target in the HPV cancers. However, two mitotic inhibitors, the Plk1 inhibitor, BI-2536 and paclitaxel showed no selectivity between the HPV-positive and -negative cell lines (Supplementary Fig. S3), suggesting a more specific mechanism may be responsible for the HPV-mediated sensitivity.

HPV cancer cell lines are highly sensitive to inhibition of Aurora A kinase *in vitro* and *in vivo*

To validate the Aurora kinases as selective targets in HPV-driven cervical cancer, we assessed the activity of well-characterized inhibitors of Aurora A and B. The Aurora B inhibitor ZM447439 (18) was not selective for the HPV lines (Supplementary Fig. S4). The potent, orally active inhibitor of Aurora A kinase, MLN8237/

Alisertib (19) was investigated in a panel of HPV-transformed cervical cancer cell lines. HeLa, CaSki, and ME180 (HPV18/38) were highly sensitive to Alisertib with IC_{50} values of less than 1 μmol/L, whereas SiHa were less sensitive with an IC_{50} of 1.2 μmol/L (Fig. 2A and Supplementary Table S3). The non-HPV cervical cancer cell lines HT3 and C33A were less sensitive with an IC_{50} value of 2 and 16 μmol/L, respectively (Fig. 2B and Supplementary Table S3). We also tested a panel of squamous cell carcinoma (SCC) cell lines to increase the number of non-HPV cancer cell lines from a keratinocyte origin. These were significantly less sensitive to Alisertib with IC_{50} values above 5 μmol/L in all cases (Fig. 2C). The difference in drug sensitivity was not a consequence of different proliferative rates, as all cell lines tested had a similar doubling time. The sensitivity of the HPV-cervical cancer cell lines are clinically relevant as plasma concentrations of 1 to 5 μmol/L of Alisertib have been reported in patients (20).

To assess the ability of Alisertib to inhibit tumor growth in vivo, nude mice were injected s.c. with either HeLa (HPV16), CaSki (HPV18), or C33A (non-HPV) lines. When tumors had formed and were palpable, Alisertib treatment (orally, 30 mg/kg daily for

10 days) was initiated. The non-HPV C33A tumors showed an initial inhibition of growth that continued to 10 days after the final treatment, but tumor growth recovered to control levels thereafter. By contrast, HeLa and CaSki tumors reached approximately 20 to 35 mm³ during the treatment phase then regressed with Alisertib treatment, with no signs of tumor at day 50 after treatment (Fig. 3A), and excision of the original site of inoculation showed no residual tumor.

We also assessed a transgenic model of HPV16 E7–dependent precancer using a skin graft model. In this model, donor mice have HPV16 E7 expression controlled by the keratin 14 promoter (K14E7) resulting in E7 expression in squamous epithelial keratinocytes, driving hyperplasia of the keratinocytes (21). Grafting of skin from either wild-type or K14E7 mice onto a syngeneic host results in well-healed grafts (22). Mice with well-healed grafts underwent two cycles of 10-day Alisertib treatment, and the mice where then sacrificed and the grafts harvested for immunohistochemical analysis. This treatment resulted in swelling and reddening of the K14E7 grafts only. In Alisertib-treated E7 grafts, we observed a significant increase in apoptotic cells compared with untreated E7 grafts (Fig. 3B). No apoptotic cells were detected in the adjacent wild-type grafts. There was also an increase in the number of mast cells immediately adjacent to the epidermis in the Alisertib treated E7 grafts compared with both the adjacent wild-type grafts and untreated E7 grafts (Fig. 3C and Supplementary Fig. S5), likely to be in part responsible for the increased swelling of the Alisertib-treated E7 grafts.

Treatment with Alisertib induces polyploidy and cell death in HPV-transformed cervical cancer cell lines.

Cell-cycle progression was analyzed in cells after Alisertib treatment by flow cytometry. Treatment of cells with 5 μmol/L Alisertib for 24 hours resulted in increased cells with 4N and >4N DNA and a reduction in the 2N and S phase population in all cell lines (Fig. 4A; Supplementary Figs. S6 and S7A). There was an increase in the sub-diploid population (<2N) in a time-dependent manner in all cell lines, which was more pronounced in HPV-transformed cells. After 72 hours of treatment, 3 of the 4 HPV-transformed showed high sub-diploid population (HeLa, 70%; Caski and ME180, 75%) indicating cell death. The exception was SiHa, where the sub-diploid population was 36%. By contrast, the two non-HPV cancer cell lines, C33A and HT3, demonstrated lower sub-diploid populations of 14% and 31%, respectively, but accumulated cells with high polyploidy (>4N) suggesting a failed cytokinesis, but this did not result in cell death.

To confirm that the induction of 4N and >4N DNA content was a consequence of failure of cytokinesis, all cell lines were subject to immunofluorescence staining of the microtubule cytoskeleton with anti–α-tubulin and DAPI for DNA (Supplementary Fig. S7B). The percentage of binuclear and multinuclear cells 1 and 2 days after Alisertib treatment increased to a similar level in all cells (Supplementary Fig. S7C). Together, these data suggest that the accumulation of cells with 4N or greater DNA content was indeed a consequence of failure of cytokinesis, but only in HPV-transformed cells did this result in a significant loss of viability.

The effects of Alisertib on cell viability were confirmed using time-lapse microscopy. In all cell lines, drug treatment caused cells to arrest in mitosis (rounded mitotic morphology), and undergo failed cytokinesis (producing single daughter cells). However, apoptosis was prominent in the HPV-transformed cell lines (Supplementary Fig. S8). Analysis of the timing of cell death in
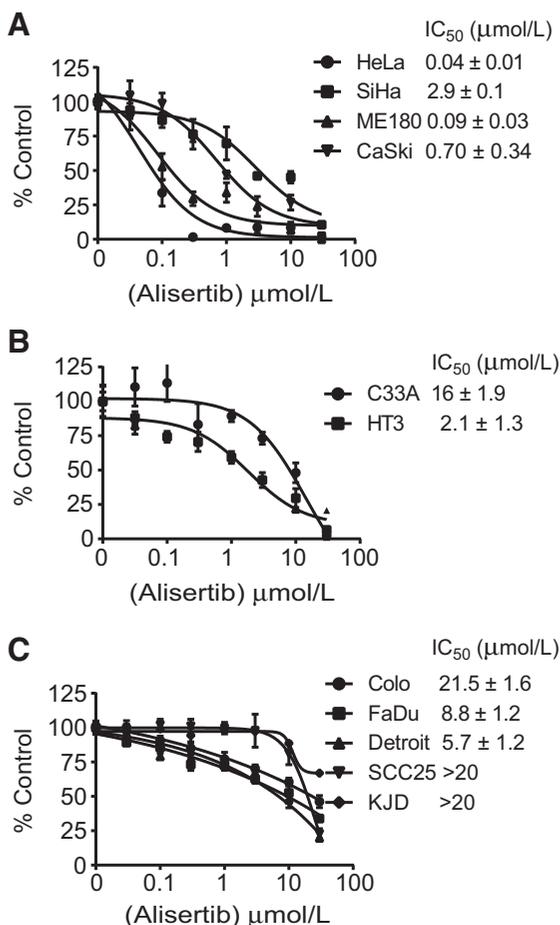

Figure 2.
HPV-transformed cancer cell lines are more sensitive to Alisertib than non-HPV cancer cells. Dose–response curves and IC_{50} values generated for Alisertib on a panel of HPV (A), non-HPV (B), and SCC (C) cancer cell lines using cell viability (resazurin) as the readout. The IC_{50} values calculated from four replicates are shown.

Figure 3.
Alisertib selectively targets HPV E7-expressing cells in two mouse models. A, groups of 6 mice were injected with either CaSki (HPV16), HeLa (HPV18), or C33A (non-HPV) cervical cancer cells s.c. in one flank of each mouse. In each group, mice were treated with 30 mg/kg Alisertib or carrier for 10 consecutive days and then followed up daily until culled, with the control-treated group culled when the tumor size reached 500 to 600 mm^3. The bar indicates the time of treatment. B, groups of 7 mice, with well-healed grafts of either wild-type or K14E7 skin were treated with or without two 10-day cycles of Alisertib as described for the xenograft experiments. Formalin-fixed, paraffin-embedded samples were immunostained for cleaved caspase-3. The number of cells stained was scored visually by microscopy. The number of cells in 10 ×20 fields from each mouse are shown. C, skin sections from B were stained for mast cells, and the numbers of mast cells immediately adjacent to the epidermis were counted in five ×20 fields; *, $P > 0.05$.
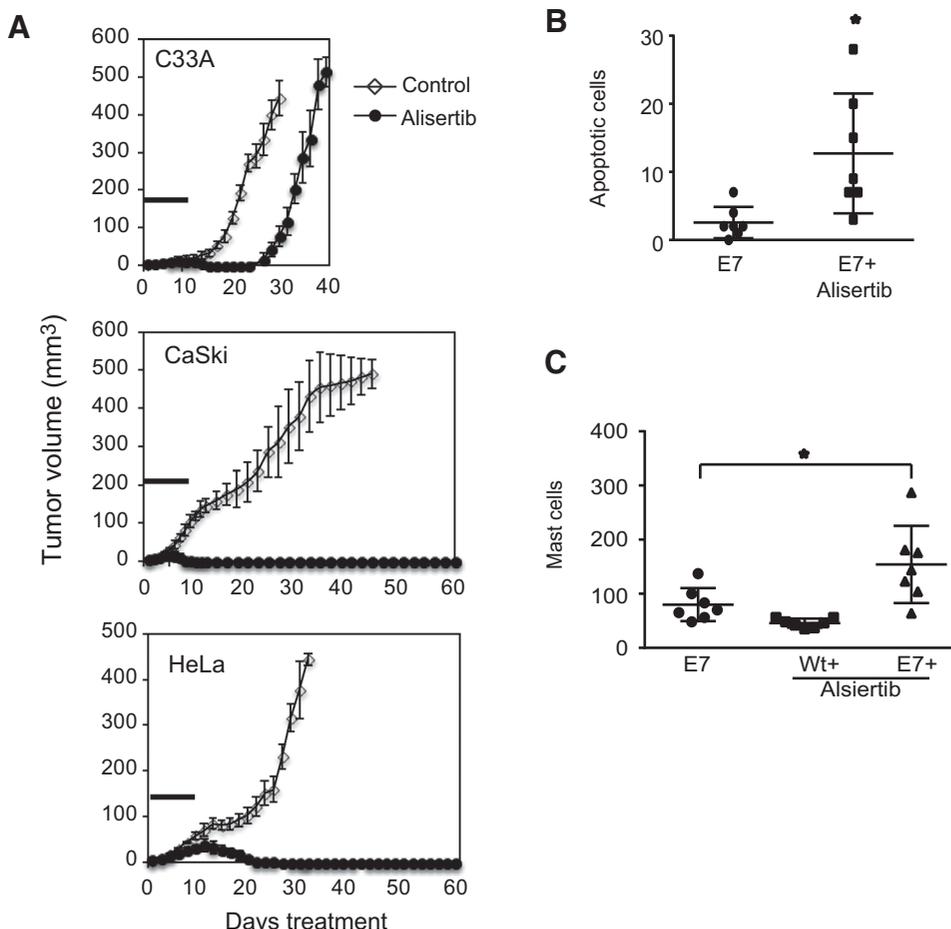
the HPV-transformed cell lines showed that 50% to 60% of cells underwent two rounds of mitosis before triggering cell death quickly, whereas a further 20% required a single mitosis, but then death was delayed for >20 hours (Supplementary Fig. S9). Surprisingly, the length of mitotic arrest induced by the drug was up to 5 times longer in the HPV-transformed lines (Fig. 4B). Aurora A inhibition normally results in a relatively short mitotic delay then exit into failed cytokinesis (23–25). Our data suggest a unique sensitivity in cells where HPV is present that results in a highly extended mitotic arrest.

Mechanism of Alisertib-induced death in HPV cancer cell lines

To examine the apoptosis induced by Alisertib treatment, HeLa cells overexpressing either Bcl-2 or Mcl-1 were assessed for their sensitivity to Alisertib. Etoposide and taxol were used as respective positive controls. The Mcl-1-HeLa cells were highly resistant to Alisertib compared with the parental HeLa, with a >50-fold increase in IC$_{50}$ (90 nmol/L–4.7 µmol/L). Interestingly, Bcl-2 overexpression had a more modest effect on sensitivity to Alisertib (Fig. 5A). Mcl-1 and Bcl-2 overexpression was protective against taxol and etoposide, respectively (Supplementary Fig. S10), suggesting Alisertib functions via an Mcl-1–sensitive apoptotic mechanism.

A panel of apoptotic components was examined by immunoblotting of the HPV-transformed cervical cancer cell lines after 24, 48, and 72 hours of Alisertib treatment. The level of full-length PARP decreased with a concomitant increase in cleaved PARP in all HPV cell lines tested by 48 hours drug treatment. This was not detected in the non-HPV C33A line (Fig. 5B and Supplementary Fig. S11). The increased PARP cleavage was associated with an increase in the cleavage and activation of caspase-3. The levels of the antiapoptotic Mcl-1, Bcl-2, and Bcl-Xl proteins varied between each cell line. Alisertib treatment had little effect on the levels of Bcl-2 and Bcl-Xl, but there was up to 50% reduction in the level of Mcl-1 in three of the HPV-transformed lines. Alisertib treatment had little effect on either the relatively insensitive SiHa or the non-HPV C33A line. Tumor-suppressor p53 was only readily detectible by immunoblotting in the non-HPV cell lines and was not restored in the HPV-transformed lines by Alisertib treatment. The expression of p53-regulated proapoptotic proteins PUMA, NOXA, and BAD was not affected by Alisertib treatment. An increase in the level of the Mcl-1–selective BIM in the majority of cell lines treated was observed (Fig. 5B and C). The consistently reduced level of Mcl-1 in the Alisertib-treated HPV-transformed cell lines together with the increased level of BIM and the resistance to Alisertib of HeLa cells overexpressing Mcl-1 indicates that the reduced Mcl-1 and increased BIM levels are the mechanism by which apoptosis is induced by Alisertib treatment.

Aurora A inhibition targets host interaction with HPV E7

To determine whether Alisertib sensitivity was a direct consequence of expression of HPV oncogenes, C33A non-HPV cervical cancer and SCC25 non-HPV SCC cell lines were transfected with HPV16 E7 oncogene, then assessed for their sensitivity to Alisertib. Expression of E7 in SCC25 cells (SCC25-HPV16-E7)
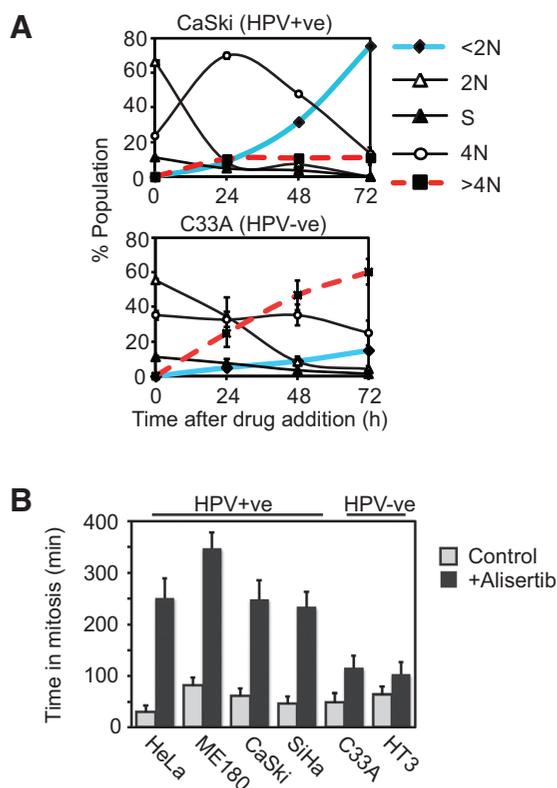
Gabrielli et al.

Figure 4.
Alisertib treatment of HPV-transformed cancer cells promotes apoptosis and delays HPV-transformed cells in mitosis. A, HPV-transformed cancer cells were treated with 5 µmol/L Alisertib and sampled at intervals over 72 hours and analyzed by flow cytometry for DNA content. The data are the mean and SD of three independent experiments. The data for only CaSki and C33A are shown. See Supplementary Figs. S6A and S12 for other cell lines. ME180 and C33A cell line data are shown in Supplementary Fig. S4. B, quantitation of the time in mitosis for each cell line with and without 5 µmol/L Alisertib treatment determined from the time-lapse experiments. The data are the mean and 95% confidence interval for >100 cells in each case.

resulted in >30-fold reduction of the IC_{50} value (from >15 to 0.5 µmol/L) whereas E7 expression in C33A cells (C33A-HPV16-E7) resulted in approximately 50% IC_{50} reduction (Fig. 6A and Supplementary Fig. S12), indicating that E7 expression induces the observed sensitivity. Our previous experiments hint that the level HPV E7 expression appeared to be correlated with sensitivity to Alisertib as the lowest E7-expressing line, SiHa (26) was the least sensitive (Fig. 2). To assess whether the level of HPV E7 expression influences Alisertib sensitivity, SCC25 lines were transduced with lentivirus HPV18 E7 as an IRES GPF labeled expression construct. The resultant population was FACS sorted into low and high GFP expression as a direct marker of HPV E7 expression (Supplementary Fig. S13; ref. 14). These populations where treated with 5 µmol/L Aliserib, and the delay in mitosis and changes in apoptotic proteins assessed as before. We observed a dose-dependent increase in mitotic delay between the low and high-expressing cells upon Alisertib treatment (Fig. 6B), which was highly significant ($P < 0.005$) in the E7 high-expressing population. Increased BIM levels were observe in all Alisertib-treated population, but a reduced Mcl-1 level (to 50% control) was only observed in E7 high-expressing population at 3 days,

correlated with decreased full-length PARP (Fig. 6C). These data together indicate that the expression of HPV E7 is responsible for the increased sensitivity of the HPV-transformed cell lines, and that the level of HPV E7 expression is an important determinant of sensitivity to Alisertib.

Discussion

Here, we have used siRNA kinome screening to identify Aurora A as a molecular target for killing HPV-driven cervical cancer cells. Previously, shRNA-based kinome screens from the Harlow and
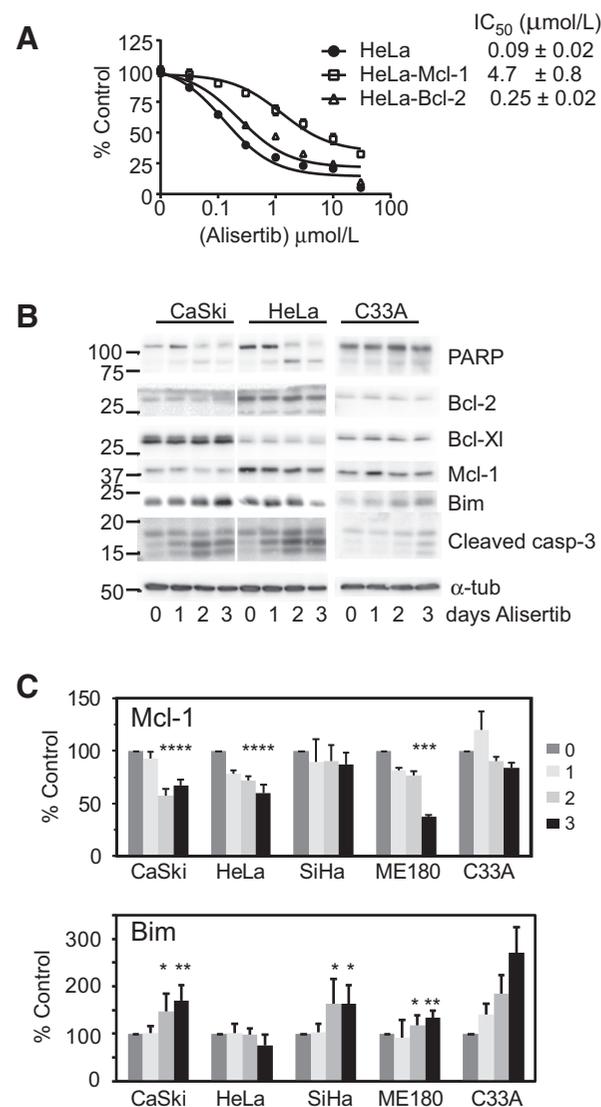

Figure 5.
Mcl-1 overexpression reduced sensitivity to Alisertib. A, dose response of parental, Bcl-2– and Mcl-1–overexpressing HeLa cells to Alisertib. The IC_{50} values for each from four determinations are shown. B, the indicated cell lines were treated with 5 µmol/L Alisertib for up to 3 days. Cells were lysed and immunoblotted for the indicated apoptotic proteins. These data are representative of three independent experiments. C, quantitation of the Mcl-1 and BIM levels from at least three independent experiments similar to that shown in B. The levels are normalized to the day 0 control for each cell line; *, $P > 0.05$; **, $P > 0.01$ compared with control.
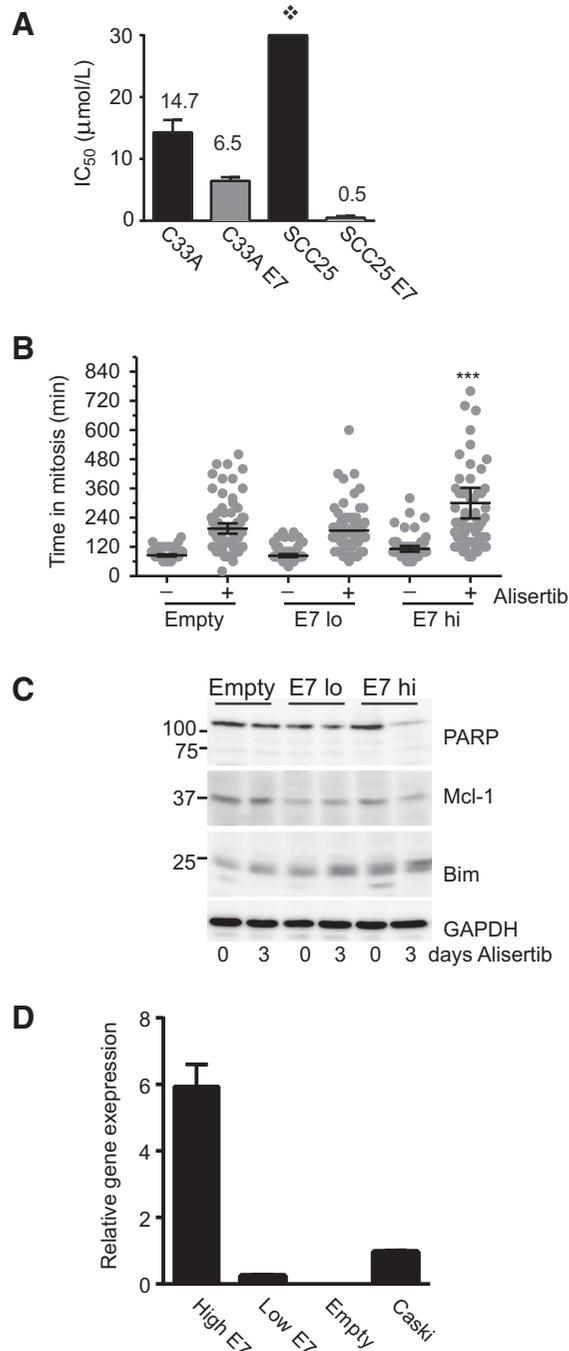
Figure 6.
Expression of HPV E7 is sufficient to sensitize cells to Alisertib. A, IC$_{50}$ values for the parental and HPV16 E7-expressing C33A and SCC25 cell lines determined from four replicate experiments. Example curves used to derive the combined data are shown in Supplementary Fig. S13. B, quantitation of the time in mitosis for each SCC25 cell lines transduced with different levels of HPV E7 with and without 5 mmol/L Alisertib treatment determined from time-lapse experiments. The data are the mean and 95% confidence interval for >100 cells in each case. ***, $P < 0.005$ compared with the empty vector control using one way ANOVA. C, SCC25 cell lines were transduced with different levels of HPV E7 and were treated with 5 mmol/L Alisertib for up to 3 days. Cells were lysed and immunoblotted for the indicated apoptotic proteins. D, the level of HPV E7 transcript expression is shown relative to CaSki.

Munger laboratories have explored the role of E7 synthetic lethality, but only 100 kinases were screened and these did not include any of our seven top hits (27).

The Aurora A inhibitor, Alisertib, has been used in over 35 clinical trials; however, it has so far only elicited modest responses in range of tumor settings (20, 28, 29). Targeting Aurora A using Alisertib demonstrated selectivity for HPV-transformed cancer cells both *in vitro* and *in vivo*. *In vitro*, the major difference observed was that the HPV cell lines failed cytokinesis and died whereas non-HPV cervical cancer lines failed cytokinesis but remained viable. In xenograft experiments, we observed that non-HPV cervical cancer was somewhat sensitive to Alisertib treatment, showing delayed tumor growth and eventual recovery, a typical response reported for Alisertib in other cancer models (30, 31). By contrast no tumor was detectable in either HeLa or CaSki cells, even 50 days after treatment. Although Alisertib had a more modest effect in mouse *K14E7* grafted model, the lack of effect on the adjacent wild-type graft demonstrates the same selectivity observed in the cancer models. The increased apoptosis and mast cell infiltrate point to Alisertib treatment having an HPV-E7–directed effect even in this premalignant setting. Together, these data provide strong evidence that Aurora A selectively targets HPV E7–expressing cells *in vitro* and *in vivo*.

This observation is supported by the mechanistic studies, which shows Aurora A depletion/inhibition selectively kills HPV-transformed cervical cancer cell, and this is dependent on HPV E7 expression. The expression HPV E7 in HPV-negative C33A and SCC25 sensitized them to Alisertib and the level of E7 correlated with sensitivity. HPV E7 expression has been reported to increase Aurora A levels (32), though we found little difference in the level of Aurora A in HPV and non-HPV cancer cell lines. HPV E7 can upregulate the expression of the p53-related p73 protein via dysregulated E2F activity, which can transactivate the expression of the proapoptotic proteins PUMA and NOXA. Aurora A has been reported to phosphorylate p73, an HPV E7–regulated gene (33), and inhibit its transcriptional activity, thus inhibiting the expression of p73-regulated PUMA and NOXA-promoting apoptosis (25, 34). However, we found no evidence of this mechanism in Alisertib-dependent death in the HPV-transformed cancer cell lines.

A consistent difference between the Alisertib-treated HPV-transformed and non-HPV cell lines is the time in mitosis, with the HPV-transformed lines all delaying up to five time longer in mitosis as non-HPV cells. These data and the finding that a majority of cells required transit through one or two mitoses before undergoing apoptosis suggested that the extended mitotic delay was a major contributor to the selective killing observed. A number of components of the apoptotic pathway have been reported to be regulated by mitosis. Mcl-1 is destabilized by CDK1–Cyclin B (35, 36), and BIM, an Mcl-1–selective BH3-only protein (37), is phosphorylated by Aurora A, which promotes its degradation in mitosis. Our data indicate that the apoptosis promoted by Alisertib treatment in the HPV-transformed cells is dependent on Mcl-1. The mechanism by which Aurora A regulates Mcl-1 stability is linked to the increased delay in mitosis found with Aurora A inhibition in the HPV-transformed cells. The longer delay in mitosis increases the destruction of Mcl-1. In addition to this reduction in antiapoptotic signal, inhibition of Aurora A directly stabilizes BIM, increasing proapoptotic signalling. Others have shown that BIM depletion reduced the sensitivity of HeLa cells to Aurora A inhibitor (38), supporting the role for BIM in this

Gabrielli et al.

apoptotic signalling. The combined effect of reduced Mcl-1 and maintenance of BIM levels, which bound by Mcl-1, results in elevated BIM not bound in an antiapoptotic Mcl-1 complex. The degree of Mcl-1destruction during the mitotic delay may be the factor determining whether one or two mitoses are required for triggering apoptosis, as observed in the time lapse experiments. CDK1–Cyclin B phosphorylation of BCL-2 and Bcl-Xl has also been reported to inhibit their antiapoptotic activity (39), and the combined effect of reduction of antiapoptotic Bcl-2, Bcl-Xl, and Mcl-1, with maintenance of BIM levels promoting an overall proapoptotic signal.

It may be that the level of E7 expression directly influences CDC20 expression and thereby Mcl-1 stability in mitosis. The level of HPV E7 expression contributes to length of the mitotic delay in Alisertib-treated cells. Low level E7 expression had little effect on time of E7 transduced SCC25 cells in mitosis with Alisertib treatment, but high-level expression in these cells delayed significantly extended the mitotic delay. Only the high-level HPV E7–expressing SCC25 cells showed significant reduction in Mcl-1 levels, consistent with this proposal. The mechanism underlying the effect of Aurora A inhibition in the E7 expressing cells is at present unknown. In summary, we have identified inhibition of Aurora A as a synthetic lethal target in the presence of the HPV E7 oncogene and demonstrated that inhibiting Aurora A with the small-molecule inhibitor Alisertib selectively and effectively targets HPV E7–expressing cells in vivo. The data presented here demonstrate that targeting Aurora A with drugs such as Alisertib may be an effective therapy for recurrent cervical cancer, and may be useful in treating other HPV-transformed cancer types.

Disclosure of Potential Conflicts of Interest

No potential conflicts of interest were disclosed.

Authors' Contributions

Conception and design: B. Gabrielli, F. Bokhari, M.V. Ranall, N.A.J. McMillan
Development of methodology: B. Gabrielli, F. Bokhari, M.V. Ranall, A.J. Stevenson, M. Shaikh, D. Clarke, P. Leo, D. Skalamera, T.J. Gonda, N.A.J. McMillan

References

1. Forman D, de Martel C, Lacey CJ, Soerjomataram I, Lortet-Tieulent J, Bruni L, et al. Global burden of human papillomavirus and related diseases. Vaccine 2012;30:F12–23.
2. Walboomers JM, Jacobs MV, Manos MM, Bosch FX, Kummer JA, Shah KV, et al. Human papillomavirus is a necessary cause of invasive cervical cancer worldwide. J Pathol 1999;189:12–9.
3. zur Hausen H. Papillomavirus infections-a major cause of human cancers. Biochim Biophys Acta 1996;1288:F55–78.
4. Chaturvedi AK, Engels EA, Pfeiffer RM, Hernandez BY, Xiao W, Kim E, et al. Human papillomavirus and rising oropharyngeal cancer incidence in the United States. J Clin Oncol 2011;29:4294–301.
5. Parkin DM, Bray F. Chapter 2: the burden of HPV-related cancers. Vaccine 2006;24:S3/11–25.
6. Schiller JT, Castellsague X, Garland SM. A review of clinical trials of human papillomavirus prophylactic vaccines. Vaccine 2012;30: F123–38.
7. Tabrizi SN, Brotherton JM, Kaldor JM, Skinner SR, Liu B, Bateson D, et al. Assessment of herd immunity and cross-protection after a human papillomavirus vaccination programme in Australia: a repeat cross-sectional study. Lancet Infect Dis 2014;5:70841–2.
8. Stern PL, van der Burg SH, Hampson IN, Broker TR, Fiander A, Lacey CJ, et al. Therapy of human papillomavirus-related disease. Vaccine 2012;30: F71–82.
9. Scheffner M, Werness BA, Huibregtse JM, Levine AJ, Howley PM. The E6 oncoprotein encoded by human papillomavirus types 16 and 18 promotes the degradation of p53. Cell 1990;63:1129–36.
10. Moody CA, Laimins LA. Human papillomavirus oncoproteins: pathways to transformation. Nat Rev Cancer 2010;10:550–60.
11. DeCaprio JA. Human papillomavirus type 16 E7 perturbs DREAM to promote cellular proliferation and mitotic gene expression. Oncogene 2014;33:4036–8.
12. Ojesina AI, Lichtenstein L, Freeman SS, Pedamallu CS, Imaz-Rosshandler I, Pugh TJ, et al. Landscape of genomic alterations in cervical carcinomas. Nature 2014;506:371–375.
13. Gu W, Putral L, Hengst K, Minto K, Saunders NA, Leggatt G, et al. Inhibition of cervical cancer cell growth in vitro and in vivo with lentiviral-vector delivered short hairpin RNA targeting human papillomavirus E6 and E7 oncogenes. Cancer Gene Ther 2006;13:1023–32.
14. Skalamera D, Ranall MV, Wilson BM, Leo P, Purdon AS, Hyde C, et al. A high-throughput platform for lentiviral overexpression screening of the human ORFeome. PLoS ONE 2011;6:e20057.
15. Stevens FE, Beamish H, Warrener R, Gabrielli B. Histone deacetylase inhibitors induce mitotic slippage. Oncogene 2008;27:1345–54.
16. De Boer L, Oakes V, Beamish H, Giles N, Stevens F, Somodevilla-Torres M, et al. Cyclin A/cdk2 coordinates centrosomal and nuclear mitotic events. Oncogene 2008;27:4261–8.

17. Khairuddin N, Blake SJ, Firdaus F, Steptoe RJ, Behlke MA, Hertzog PJ, et al. In vivo comparison of local versus systemic delivery of immunostimulating siRNA in HPV-driven tumours. Immunol Cell Biol 2014;92:156–63.

18. Ditchfield C, Johnson VL, Tighe A, Ellston R, Haworth C, Johnson T, et al. Aurora B couples chromosome alignment with anaphase by targeting BubR1, Mad2, and Cenp-E to kinetochores. J Cell Biol 2003;161:267–80.

19. Manfredi MG, Ecsedy JA, Chakravarty A, Silverman L, Zhang M, Hoar KM, et al. Characterization of Alisertib (MLN8237), an investigational small-molecule inhibitor of aurora A kinase using novel in vivo pharmacodynamic assays. Clin Cancer Res 2011;17:7614–24.

20. Cervantes A, Elez E, Roda D, Ecsedy J, Macarulla T, Venkatakrishnan K, et al. Phase I pharmacokinetic/pharmacodynamic study of MLN8237, an investigational, oral, selective aurora a kinase inhibitor, in patients with advanced solid tumors. Clin Cancer Res 2012;18:4764–74.

21. Gulliver GA, Herber RL, Liem A, Lambert PF. Both conserved region 1 (CR1) and CR2 of the human papillomavirus type 16 E7 oncogene are required for induction of epidermal hyperplasia and tumor formation in transgenic mice. J Virol 1997;71:5905–14.

22. Dunn LA, Evander M, Tindle RW, Bulloch AL, de Kluyver RL, Fernando GJ, et al. Presentation of the HPV16E7 protein by skin grafts is insufficient to allow graft rejection in an E7-primed animal. Virology 1997;235:94–103.

23. Hoar K, Chakravarty A, Rabino C, Wysong D, Bowman D, Roy N, et al. MLN8054, a small-molecule inhibitor of Aurora A, causes spindle pole and chromosome congression defects leading to aneuploidy. Mol Cell Biol 2007;27:4513–25.

24. Wysong DR, Chakravarty A, Hoar K, Ecsedy JA. The inhibition of Aurora A abrogates the mitotic delay induced by microtubule perturbing agents. Cell Cycle 2009;8:876–88.

25. Katayama H, Wang J, Treekitkarnmongkol W, Kawai H, Sasai K, Zhang H, et al. Aurora Kinase-A inactivates DNA damage-induced apoptosis and spindle assembly checkpoint response functions of p73. Cancer Cell 2012;21:196–211.

26. de Boer MA, Jordanova ES, Kenter GG, Peters AA, Corver WE, Trimbos JB, et al. High human papillomavirus oncogene mRNA expression and not viral DNA load is associated with poor prognosis in cervical cancer patients. Clin Cancer Res 2007;13:132–8.

27. Baldwin A, Grueneberg DA, Hellner K, Sawyer J, Grace M, Li W, et al. Kinase requirements in human cells: V. Synthetic lethal interactions between p53 and the protein kinases SGK2 and PAK3. Proc Natl Acad Sci U S A 2010;107:12463–8.

28. Dees EC, Cohen RB, von Mehren M, Stinchcombe TE, Liu H, Venkatakrishnan K, et al. Phase I study of aurora A kinase inhibitor MLN8237 in advanced solid tumors: safety, pharmacokinetics, pharmacodynamics, and bioavailability of two oral formulations. Clin Cancer Res 2012;18:4775–84.

29. Friedberg JW, Mahadevan D, Cebula E, Persky D, Lossos I, Agarwal AB, et al. Phase II study of alisertib, a selective Aurora A kinase inhibitor, in relapsed and refractory aggressive B- and T-cell non-Hodgkin lymphomas. J Clin Oncol 2014;32:44–50.

30. Do TV, Xiao F, Bickel LE, Klein-Szanto AJ, Pathak HB, Hua X, et al. Aurora kinase A mediates epithelial ovarian cancer cell migration and adhesion. Oncogene 2014;33:539–49.

31. Zhou N, Singh K, Mir MC, Parker Y, Lindner D, Dreicer R, et al. The investigational Aurora kinase A inhibitor MLN8237 induces defects in cell viability and cell-cycle progression in malignant bladder cancer cells in vitro and in vivo. Clin Cancer Res 2013;19:1717–28.

32. Spardy N, Covella K, Cha E, Hoskins EE, Wells SI, Duensing A, et al. Human papillomavirus 16 E7 oncoprotein attenuates DNA damage checkpoint control by increasing the proteolytic turnover of claspin. Cancer Res 2009;69:7022–9.

33. Brooks LA, Sullivan A, O'Nions J, Bell A, Dunne B, Tidy JA, et al. E7 proteins from oncogenic human papillomavirus types transactivate p73: role in cervical intraepithelial neoplasia. Br J Cancer 2002;86:263–8.

34. Dar AA, Belkhiri A, Ecsedy J, Zaika A, El-Rifai W. Aurora kinase A inhibition leads to p73-dependent apoptosis in p53-deficient cancer cells. Cancer Res 2008;68:8998–9004.

35. Harley ME, Allan LA, Sanderson HS, Clarke PR. Phosphorylation of Mcl-1 by CDK1-cyclin B1 initiates its Cdc20-dependent destruction during mitotic arrest. Embo J 2010;29:2407–20.

36. Tunquist BJ, Woessner RD, Walker DH. Mcl-1 stability determines mitotic cell fate of human multiple myeloma tumor cells treated with the kinesin spindle protein inhibitor ARRY-520. Mol Cancer Ther 2010;9:2046–56.

37. Chen L, Willis SN, Wei A, Smith BJ, Fletcher JI, Hinds MG, et al. Differential targeting of prosurvival Bcl-2 proteins by their BH3-only ligands allows complementary apoptotic function. Mol Cell 2005;17:393–403.

38. Moustafa-Kamal M, Gamache I, Lu Y, Li S, Teodoro JG. BimEL is phosphorylated at mitosis by Aurora A and targeted for degradation by betaTrCP1. Cell Death Differ 2013;20:1393–403.

39. Terrano DT, Upreti M, Chambers TC. Cyclin-dependent kinase 1-mediated Bcl-xL/Bcl-2 phosphorylation acts as a functional link coupling mitotic arrest and apoptosis. Mol Cell Biol 2010;30:640–56.

AACR American Association for Cancer Research

Molecular Cancer Therapeutics

Aurora A Is Critical for Survival in HPV-Transformed Cervical Cancer

Brian Gabrielli, Fawzi Bokhari, Max V. Ranall, et al.

Updated version	Access the most recent version of this article at: doi:10.1158/1535-7163.MCT-15-0506
Supplementary Material	Access the most recent supplemental material at: http://mct.aacrjournals.org/content/suppl/2015/10/29/1535-7163.MCT-15-0506.DC1

Cited articles	This article cites 39 articles, 16 of which you can access for free at: http://mct.aacrjournals.org/content/14/12/2753.full#ref-list-1
Citing articles	This article has been cited by 4 HighWire-hosted articles. Access the articles at: http://mct.aacrjournals.org/content/14/12/2753.full#related-urls

E-mail alerts	Sign up to receive free email-alerts related to this article or journal.
Reprints and Subscriptions	To order reprints of this article or to subscribe to the journal, contact the AACR Publications Department at pubs@aacr.org.
Permissions	To request permission to re-use all or part of this article, use this link http://mct.aacrjournals.org/content/14/12/2753. Click on "Request Permissions" which will take you to the Copyright Clearance Center's (CCC) Rightslink site.